Journal of Modern Technology and Engineering
Vol.3, No.3, 2018, pp.217-227

RECYCLABLE COMPOSITE FOR EFFICIENT NITRATE REMOVAL AND ITS APPLICATION INTO ENVIRONMENTAL WATER SAMPLES

Dalal Z. Husein[1*], T. Al-Radadi[2], Y. Denashb[2]

[1]Department of Chemistry, Faculty of Science, Assiut University, Alkharga, Egypt
[2]Faculty of Science, King Abdul-Aziz University, Jeddah, Saudi Arabia

Abstract. High nitrate concentrations in surface water bodies can pose a threat to human health. To reduce nitrate concentration in aqueous bodies, a hybrid composite adsorbent was prepared and characterized using FTIR and SEM analysis. The absorptive properties of the prepared hybrid composite towards nitrate removal was investigated using fixed bed mode in terms bed height, flow rate and initial nitrate concentration effects. Different breakthrough curves were applied using Thomas, Adams-Bohart, and Yoon- Nelson dynamic models to find out the best model describing the adsorption dynamics in fixed column. Three environmental samples from King Abdulaziz University Wastewater treatment plant, Jeddah Lake and Red sea near Jeddah coast, were used as representations for wastewater, brackish water and saline water, to validate the ability of the prepared hybrid composite to remove the nitrate ions from aquatic bodies.

Keywords: nitrate, adsorption, fixed bed, environmental samples.
Corresponding author: Husein Dalal, Assiut University, New Valley branch-Alkharga, P.O. box.72511, Egypt, Fax: 0020927937576, e-mail: *dalal_husein@yahoo.com*
Received: 13 October 2018; Accepted: 12 November 2018; Published: 07 December 2018.

1 Introduction

Nitrate is a major nutrient required for plant growth, but excessive of nitrate results in eutrophication of aquatic bodies affecting the aquatic environment and causes harm to people's health and animals. High nitrate contents in ground and surface water, as a result of the disposal of untreated municipal and industrial wastes and excessive use of nitrogenous fertilizers, are a serious global environmental problem (Ansari & Parsa, 2016). Drinking water of elevated nitrate concentration can potentially cause blue baby syndrome in infants (Liu et al., 2018) and stomach cancer in adults. Furthermore, elevated concentrations of nitrate in water and feed lead to reduced vitality and slow weight gain in livestock (Chiu et al., 2007). Nitrate removal from water, by conventional methods, includes two main sets of treatment processes: physicochemical and biological (Demiral & Gunduzoglu, 2010). Biological technique is favored in the treatment of high nitrate contents. However, it is difficult to keep the biological processes at their optimum conditions (Chabani et al., 2006). The most traditional physicochemical techniques for nitrate removal are ion exchange (Boumediene & Achour, 2004), electrodialysis (Elmidaoui et al., 2001), ultrafiltration (Zhu et al., 2006), denitrification (Soares, 2000), and adsorption (Tofighy & Mohammadi, 2012). From the point of view of economy and efficiency, adsorption process is very practicable for in situ treatment of ground and surface water. This is because of its ease of application. As adsorbent is the core of the adsorption technology, efforts should be directed to find novel, efficient and low cost adsorbents. Several adsorbents including those which are carbon-based, naturally occurring, industrial wastes, agricultural wastes, ion exchange resins,

biosorbents and other synthetic inorganic and organic compounds have been used to remove nitrate from water (Jones et al., 2015; Olfs et al., 2009; Alves et al., 2015; Afkhami et al., 2007; Fu et al., 2009; Frison et al,. 2013). Most of these adsorbents have low removal efficiency because of their limited adsorption capacities (Husein, 2013). Lately, more trials have been made to modify the surface of adsorbents so that their adsorption capacities improved. In view of abovementioned motivations, nitrate removal from wastewater becomes vital to preserve human health and the environment. Thus, the purpose of this study is to explore the applicability of new composite derived from the used papers for the removal of nitrate from aqueous solution and environmental samples.

2 Materials and methods

2.1. Instrumentation, adsorbent preparation and adsorption design

The equipments used in this work are: Ion Chromatograph (ICS: 900, Dionex, USA), inductively coupled plasma-atomic emission spectrometer (ICP-OES Optima 4100 DV, Perkin Elmer, USA), FTIR spectrophotometer (Jasco model FT-IR 310, Japan), Scanning electron microscope, SEM, (JEOL. JSM 6360 CityplaceLV), domestic microwave oven (Samsung, 2450MHz, 800W). All chemicals or reagents used in this work were purchased from BDH Co. Nitrate stock solution, $500mg/L$; was prepared by dissolving $0.6853g$ of $NaNO_3$ in $1L$ of de-ionized water. The pH of the influent nitrate solution was adjusted by adding small drops of either $0.1MHCL$ or $0.1M\ NaOH$ solution. The preparation of hybrid composite beads (HCB) is mentioned elsewhere (Husein et al., 2016). In brief: $50g$ used papers were treated with $2L\ 1N\ NaOH$ then subjected to microwave radiation for $15min$. After several washing with deionized water, one liter of $1000mg/L\ Zr(IV)$ is added to the wet residue. After $48h$, the residue was filtered and dried at60^0C. Six grams of material was stirred with $10g$ sodium alginate that dissolved in $300mL$ deionized for $15min$. The composite slurry pumped into a solution of $0.1M\ CaCl_2$ under continuous stirring then rinsed and dried at oven at 60^0C. Column with an inner diameter of $1.2cm$ and a length of $40cm$ was used for fixed bed studies. The desired quantity of dried hybrid composite beads (HCB) derived from papers was allowed to swell under deionized water before column backing. The average size of swollen hybrid beads was increased by 320%. Nitrate solution was injected into the column in downward direction. To investigate the effect of flow rate on nitrate adsorption, the influent nitrate concentration was held constant at $30mg/L$, and the flow rate was 3, 6 and $10mL/min$, respectively. The bed height and pH were kept constant at $1.6cm(0.2)$ and 2.36, respectively. Different bed heights of 1.6, 3.2 and $4.8cm$ were used and the effect on the column performance was analyzed. The initial inlet concentration and flow rate were maintained at 30 mg/L and 6 mL/min. The initial concentration of nitrate was performed using 20, 30 and $60mg/L$ and keeping a bed depth of $1.6cm$ and flow rate of $6mL/min$.

2.2. Analysis of fixed bed adsorption data

All fixed-bed columns were operated until the nitrate outlet column concentration (C_t) was 95% of the influent concentration C_0. The treated nitrate effluent volume $V_{eff}(mL)$ was determined using the relation:

$$V_{eff} = Q \times t_{total}, \tag{1}$$

where Q is the nitrate volumetric flow rate (mL/min) and t_{total} is the exhaustion time (min). The maximum column capacity $q_{total}(mg)$ for nitrate anions can be obtained from the area under the breakthrough curve as:

$$q_{total} = \frac{Q}{1000} \int_{t=0}^{t=total} C_{ad}dt, \tag{2}$$

where C_{ad}, mg/L , is the concentration of nitrate removal (mg/L) can be found from the difference between influent and effluent nitrate concentrations. The maximum adsorption capacity of the hybrid composite beads q_e (mg/g) used in the column is defined as:

$$q_e = {}^{q_{total}}\!/_{m}, \tag{3}$$

where m is the total amount of the HCB material (g) in the column. The total amount of nitrate sent to the column, m_{total} (mg) was estimated using the following relation:

$$m_{total} = {}^{C_0 Q t_{total}}\!/_{1000}. \tag{4}$$

The column performance, $Y\%$, can be evaluated in percentage by the ratio in the following relation:

$$Y^{\%} = \left({}^{q_{total}}\!/_{m_{total}}\right) \times 100. \tag{5}$$

The flow rate represents the empty bed contact time (EBCT) in the column, can be achieved by the mathematical expression:

$$EBCT(\text{min}) = {}^{bed\ volume\ (mL)}\!\Big/_{flowrate\ \left({}^{mL}\!/_{\text{min}}\right)}. \tag{6}$$

2.3. Application to water samples in Jeddah, Saudi Arabia

The proposed method was applied to different environmental water samples, including fresh water (saline and brackish water) and wastewater samples. The samples were collected from the places: Red sea near Jeddah coast (RS), Jeddah Lake (JL) and King Abdulaziz University Wastewater treatment plant (KWP). The collected samples were filtered through a cellulose membrane filter (0.45 μm pore size) and stored in polyethylene bottles at 5^0C, in the dark. The parameters: pH, conductivity, total suspended solids (TSS), total solids (TS), total dissolved solids (TDS), fluoride, bromide, chloride and nitrate were measured in the obtained environmental samples. The adsorption experiments were performed under natural pH by adding $0.1g$ of HCB to $50mL$ naturally nitrate occurring samples. Location map was captured using the Google Earth program, Fig. 1.

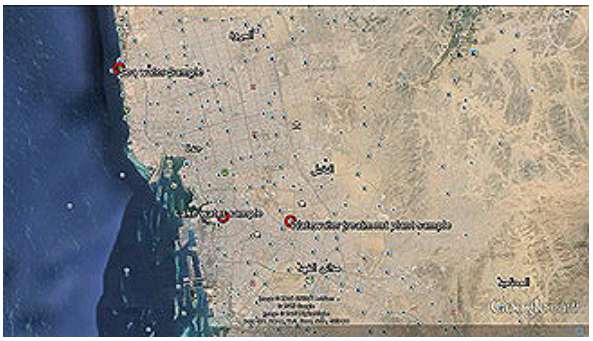

Figure 1: Location map of the collected environmental water samples

3 Results and discussions

3.1 Fourier Transform Infra Red Spectroscopy and surface morphology (SEM) analysis of HCB

The FTIR spectra of raw papers (a), alkali-bleached zirconium loaded papers (b) and the hybrid composite beads, HCB, (c), Fig. $2.a-c$, showed a characteristic peak of cellulose in the region of 1000 to $1200cm^{-1}$ while the band near $1200cm^{-1}$ related to CH_2 wagging vibrations in the cellulose. The bands at $2900cm^{-1}$ are characteristic of C-H stretching and the bands near

$3330cm^{-1}$ represented the OH vibrations. In the spectrum of the raw papers, Fig. 2.a, the band at $1500cm^{-1}$ corresponds to aromatic ring vibrations (liginin). Such band was seen to be weak in the spectrum of bleached zirconium loaded papers, Fig. 2.b. This finding indicates that $NaOH$ treatment further removed some soluble lignin in the raw papers. The band at $3339cm^{-1}1$ in the spectrum of raw papers, Fig. 2.a, was seen to be increased in intensity in spectra of both bleached zirconium loaded papers and the hybrid composite beads, Fig. 2.b and c. The small peak at $1720cm^{-1}$ in Fig. 2.a, disappeared and new peaks at around $1.600cm^{-1}$ were observed in Fig. 2.b, which indicated that free carboxylic groups of raw papers have been successfully modified by zirconium cation. Moreover, the shift of OH band from $3339cm^{-1}$ (before zirconium loading) to $3327cm^{-1}$ (after zirconium loading) may indicate that alcoholic OH groups could participate in the binding of Zr ions. Many changes have been observed after the grafting of Zr-loaded papers with alginate ions. The band at $2900cm^{-1}$ in Fig. 2.a, was seen to be split into higher intense peaks in HCB, Fig. 2.c, due to the CH aliphatic of alginate. Also, an observed increase in intensity near 3330 and $1600cm^{-1}$ in the spectrum of HCB may be attributed to OH and carboxylate salt groups in the alginate structure.

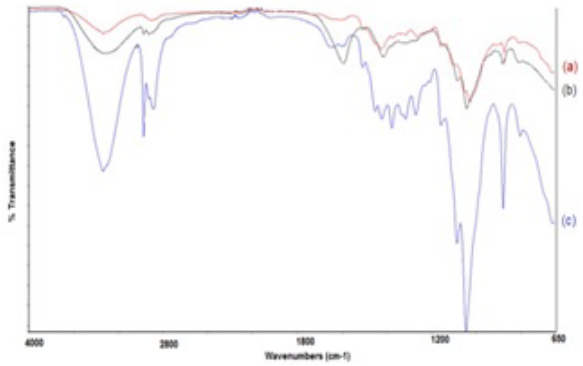

Figure 2: FTIR spectra of raw papers (a), leached zirconium loaded papers (b) and the hybrid composite beads (c).

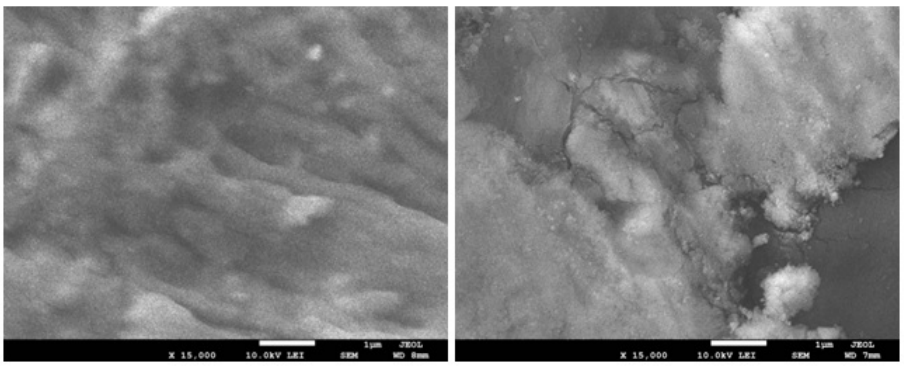

(a) (b)

Figure 3: SEM analysis of HCB: (a) before and (b) after nitrate adsorption

SEM analysis of the HCB before and after nitrate adsorption is illustrated in Fig. 3a and b. Before nitrate adsorption (Fig. 3a), the beads surface appeared as rough and have cavities. After adsorption, the beads surfaces were covered with nitrate anions leading to the formation of molecular cloud of uniform thickness and coverage (spread) whereas roughness structure disappeared, Fig. 3b.

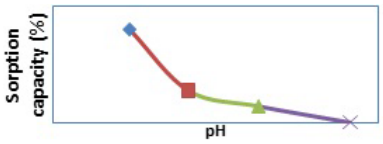

Figure 4: Effect of pH on nitrate adsorption capacity onto HCB

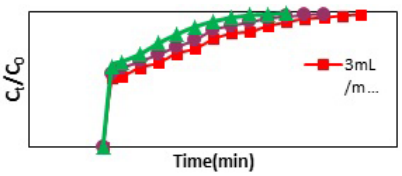

Figure 5: Breakthrough curve the flow rate effect on nitrate adsorption onto HCB

3.2 pH studies in batch mode

In the pH range 2.36-9.14, the variation of nitrate adsorption onto HCB was investigated. The contact time was enough to reach the equilibrium, Fig. 4. It is found that the amount of adsorbed nitrate increases at lower pH. This behavior is due to the excess of hydrogen ions in solution at lower pH. This increases the number of positively charged sites on HCB adsorbent surfaces, which favor the adsorption of the nitrate anions due to electrostatic attraction. The acid-base interaction between base nitrate and acid on the adsorbent surface also favors the adsorption process. According to pH analyses, $pH2.36$ is recommended to apply in the subsequent nitrate removal processes.

3.3. Column mode experiments

3.3.1. Effect of flow rate on breakthrough curve

As seen in Fig. 5, decreasing of flow rate leads to increasing of both breakthrough and exhausting points of the curve. At a low rate of influent, nitrate had more time to contact with HCB that resulted in a higher removal of nitrate ions in column (Table 1). At higher flow rate nitrate had less time to contact with the HCB bed which resulted in a steeper breakthrough curve. Thence, the adsorption efficiency decreases with an increase in flow rate due to the shorter residence time of the nitrate molecule in the fixed bed column. As conducted in Table 1, the exhaustion time and the maximum capacity decreased from 46.81 to $9.5min$ and from 4.65 to 2.62 mg/g, respectively, as the flow rate increased from 3 to 10 ml/min. In addition, the percent removal and treated volume decreased from 22.07 to 18.41%, and from 140 to 100 mL, respectively. As the influent flow rate increased from 3 to 10 ml/min, the EBCT decreased from 0.603 min to 0.181 min, and the exhaust decreased from 46.81 min to 9.50 min.

Table 1. Column data obtained for nitrate removal by HCB at different flow rates

Exp. parameters	C_0 (mg/L)	Q (ml/min)	H (cm)	t_{total} (min)	m_{total} (mg)	q_{total} (mg)	q_e (mg)	V_{eff}	$Y\%$	EBCT
flow rate	30	3	1.6	46.81	4.21	0.93	4.65	140	22.07	0.603
	30	6	1.6	19.9	3.58	0.72	3.62	120	20.24	0.301
	30	10	1.6	9.5	2.85	0.52	2.62	100	18.41	0.181
Bed height	30	6	1.6	19.92	3.59	0.72	3.62	120	20.22	0.30
	30	6	3.2	21.51	3.87	0.84	4.18	130	21.59	0.60
	30	6	4.8	24.95	4.49	1.06	5.32	150	23.67	0.90
Initial concentration	20	6	1.6	23.32	2.80	0.59	2.96	140	21.16	0.30
	30	6	1.6	19.90	3.58	0.72	3.62	120	20.24	0.30
	60	6	1.6	16.64	5.99	1.09	5.46	100	18.23	0.30

3.3.2. Effect of bed height on breakthrough curve

Fig. 6 shows that: with increasing in column bed height from 1.6 to 4.8cm, a much higher uptake efficiency of nitrate was observed for HCB adsorbent, Table 1. The increase in the nitrate uptake capacity from 3.62 to 5.32 mg/g with the increase of HCB bed height in the column is possibly due to improvement in surface properties of the hybrid composite, which provide more binding sites on the composite surface for the adsorption. The rate at which adsorption zone travels through the fixed bed decreased with the bed depth, advising that HCB beds of an increased height may be required for nitrate adsorption. The exhaustion time and percent removal of nitrate also increased.

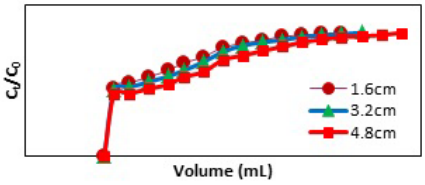

Figure 6: Breakthrough curve of the effect of bed height on the nitrate adsorption onto HCB

3.3.3. Effect of initial concentration on breakthrough curve

When the inlet nitrate anion concentration is increased for the same flow rate ($6mL/min$), the effect is a decrease in the breakthrough and exhausting time. The exhausting time decreased from 23.32 to 16.64 min, Table 1. The lower nitrate concentration gradient causes a slower transport due to decreased mass transfer coefficient or diffusion coefficient. As seen in Fig. 7, the exhausting point decreases with increasing inlet nitrate concentration whereas the sites of ion exchange and binding become speedily saturated. It can be seen that the change in the breakpoint and exhaust point time is somewhat in the same ratio as it changes in the inlet nitrate concentration. The equilibrium nitrate uptake and the total nitrate adsorbed were found to increase from 2.96 to 5.46 mg/g and from 0.59 to 1.09mg, respectively, with an increase in inlet nitrate concentration.

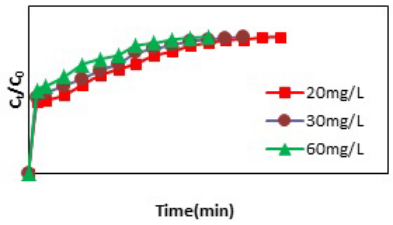

Figure 7: Breakthrough curve of the effect of initial concentration on nitrate adsorption onto HCB. Flow rate 6 ml/min, bed height 1.6 cm, pH 2.36

3.3.4 Evaluation of breakthrough curves

A breakthrough curve, the plot of effluent and influent nitrate concentration ratios (C_t/C_0) versus treated effluent volumes (V), gives the information about HCB affinity, its surface properties and the adsorption pathways (Wang et al., 2015). In this study, the adsorption data were modeled using the dynamic models presented in Table 2 at various operating conditions.

Table 2. Dynamic models used for nitrate removal onto HCB

Model	Equation*	Parameters
Thomas	$\ln(\frac{C_0}{C_t}-1)=\frac{k_{Th}q_0 m}{Q}-k_{Th}C_0 t$	kT_h, q_0
Yoon-Nelson	$\ln\frac{C_t}{C_0-C_t}=k_{YN}t-\tau k_{YN}, q_{0YN}=C_0Q_\tau/1000m$	k_{YN}, τ, q_0
Adam-Bohart	$\ln\frac{C_t}{C_0}=k_{AB}C_0 t-k_{AB}N_0\frac{Z}{F}$	k_{AB}, N_0, Z, F

k_{Th}= the Thomas rate constant ($mL/min.mg$), q_0 = the maximum adsorption capacity per g of the HCB adsorbent (mg/g), k_{YN}= the rate velocity constant (L/min), τ = the time required for 50% nitrate breakthrough (min), k_{AB}= the kinetic constant ($L/mgmin$), Z = the HCB bed depth of column, N_0= the saturation concentration (mg/L), F = the linear velocity which can be calculated by dividing the flow rate by the column section area, t= $time(min)$. When the Thomas model was applied to the experimental data, Table 3, it is found that nitrate removal by HCB fitted well to the Thomas model, whereas the observed values of R^2 are 0.99. The bed capacity, q_0,of prepared hybrid composite increased and the coefficient, K_{Th}, decreased with increase in bed height. However, as flow rate increase, K_{Th} values increase, whereas q_0 decreased. For inlet nitrate concentration, the values of both K_{Th} and q_0 decreased with increase in initial nitrate concentration. A similar trend has been reported by Yahaya et al. (2011). The well fit of the experimental data to the Thomas model revealed that both external and internal diffusion will not be the limiting step in case of nitrate removal by HCB beads (Taty-Costodes et al., 2005).

Table 3. Thomas model parameters at different conditions using linear regression analysis for nitrate removal by HCB beads

Inlet concentration	Bed height (cm)	Flow rate (mL/min)	$K_{th}(mL/min\ mg \times 10^3)$	$q_0(mg/g)$	R^2
20	1.6	6	9.05	1156.9	0.99
30	1.6	6	6.67	702.0	0.99
60	1.6	6	3.72	121.1	0.99
30	3.2	6	6.27	1354.8	0.99
30	4.8	6	5.17	2252.9	0.99
30	1.6	3	2.77	1577.7	0.99
30	1.6	10	14.43	48.5	0.99

For Yoon–Nelson dynamic model, the values of k_{YN} was found to decrease with increase in HCB bed height, whereas, the corresponding values of τ increased, Table 4. With increase in both initial nitrate concentration and influent flow rate, the k_{YN} values increased, whereas the τ values showed a reverse trend. From the Table 4, it can be seen that q_{0YN} values decreased with bed height, initial nitrate concentration and influent flow rate increasing. The R^2 values from the Yoon-Nelson model are 0.99, which indicated that this model provided a good fit for removal of nitrate by HCB.

Table 4. Yoon-Nelson model parameters at different conditions using linear regression analysis for nitrate removal by HCB adsorbent

Inlet concentration	Bed height (cm)	Flow rate (mL/min)	k_{YN} (1/min)	τ (min)	q_{0YN}	R^2
20	1.6	6	0.181	1.928	1.157	0.99
30	1.6	6	0.200	0.780	0.702	0.99
60	1.6	6	0.238	0.063	0.113	0.99
30	3.2	6	0.188	1.505	0.108	0.99
30	4.8	6	0.161	2.677	0.289	0.99
30	1.6	3	0.167	1.743	0.78	0.99
30	1.6	10	0.432	0.032	0.05	0.99

Table 5. Adam's-Bohart model parameters at different conditions using linear regression analysis for nitrate removal by HCB beads

Inlet concentration	Bed height (cm)	Flow rate (mL/min)	$K_{AB}(L/mgmin) \times 10^3$	$N_0(mg/L)$	R^2
20	1.6	6	1.500	288.252	0.91
30	1.6	6	1.033	375.357	0.92
60	1.6	6	0.543	621.937	0.91
30	3.2	6	1.057	200.483	0.92
30	4.8	6	1.027	154.971	0.92
30	1.6	3	0.500	871.821	0.92
30	1.6	10	1.827	181.705	0.90

Adam's-Bohart model assumes that the adsorption process is not instantaneous and the adsorption of nitrate onto HCB is continuous. From Table 5, it is observed that, the Adam's-Bohart rate constant, K_{AB}, decreased with increasing the nitrate concentration but increased with increasing the feed flow rate. The corresponding N_0 values were found to be decreased with the increase of HCB bed depth and influent flow rate, but increase with the increase of nitrate concentration. The regression coefficient, R^2, values in Table 5, reflect the applicability of this model for the column adsorption of nitrate onto HCB adsorbent

Overall, the used three models were well fitted for fixed bed column data, but the R^2 values from the Thomas and Yoon-Nelson models ranged from 0.98 to 0.99, which indicated that these two models provided a better fit than the Adam's-Bohart model.

3.3.5 Application of HCB to environmental samples

The water quality of three collected samples, Red sea water (RS) near Jeddah coast, Jeddah Lake (JL) and King Abdulaziz University Wastewater treatment plant (KWP) water samples is represented in Table 6. Both JL and RS are slightly alkaline while KWP is neutral. Higher nitrate content was found in KWP sample. After application of HCB to the environmental samples and soaking overnight to reach the equilibrium, the nitrate concentrations were measured and removal percentages were calculated and represented in Fig. 8. The nitrate percentage adsorbed was found to be $61.3\%, 58.7\%$ and 23.7% for RS, JL and KWP respectively. Such results indicated the suitability and efficiency of the HCB for the removal of nitrate ions from wastewater, brackish and saline water samples.

Table 6. Water quality of Red sea water (RS) near Jeddah coast, Jeddah Lake (JL) and King Abdulaziz University Wastewater treatment plant (KWP) water samples

Test	JL	RS	KWP
pH	8.07	8.14	7.2
Conductivity (ms/cm)	26.21	30.18	1.8
T.D.S (mg/L)	36.34	39.02	1.19
T.S (mg/L)	71.8	80.15	1.24
T.S.S (mg/L)	35.46	41.12	0.04
F (mg/L)	8.32	0.29	1.04
Cl (mg/L)	25446.49	4721.93	452.42
Br (mg/L)	67.82	15.97	0.63
NO_3 (mg/L)	14.11	5.02	63.58

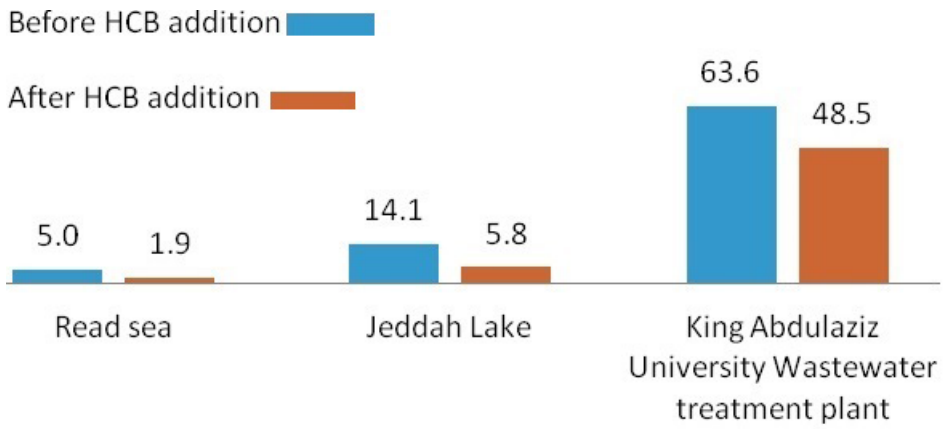

Figure 9: Nitrate concentration (mg/L) in the environmental samples before and after addition of HCB.

4 Conclusion

A practical and economical process to reduce nitrate concentrations in aqueous solutions was the major objective of this research. Used papers was bleached with alkali under microwave radiation and loaded with zirconium (IV) then reacted with alginate and converted to hybrid composite beads. The FTIR revealed that all components which are used to form alginate-zirconium/ papers composite beads are present. SEM analysis conducted that nitrate anions are strongly adsorbed by HCB. The nitrate uptake capacity increased from 3.62 to 5.32 mg/g with the increase of bed height from 1.6 to 4.8 cm. In addition, the percent removal of nitrate also increased from 20.22% to 23.67% as the bed depth increased. The percent removal and treated volume decreased from 22.07% to 18.41%, and from 140 to 100 mL as the flow rate increased from 3 to 10 ml/min. pH 2.36 was recommended to apply in the nitrate removal processes according to pH analysis. Both Thomas and Yoon-Nelson can describe the adsorption of nitrate ions onto the prepared hybrid composite beads. Application of hybrid composite beads to the three samples showed that the content of the nitrate ions was reduced dramatically upon the addition of the hybrid composite.

References

Afkhami A., Madrakian, T. & Karimi, Z. (2007). The effect of acid treatment of carbon cloth on the adsorption of nitrite and nitrate ions. *Journal of Hazardous Materials*, 144, 427–31.

Alves, C.C., Faustino, M.V., Franca, A.S. & Oliveira, L.S. (2015). Comparative evaluation of activated carbons prepared by thermo-chemical activation of lignocellulosic residues in fixed bed column studies. *IACSIT International Journal of Engineering and Technology*, 7(6),465–469.

Ansari, M. & Parsa, J.B.(2016). Removal of nitrate from water by conducting polyaniline via electrically switching ion exchange method in a dual cell reactor: Optimizing and modeling. *Separation and Purification Technology*, 169, 158–170.

Boumediene, M. & Achour, D. (2004). Denitrification of the underground waters by specific resin exchange of ion. *Desalination*, 168, 187–194.

Chabani, M., Amrane, A. & Bensmaili, A. (2006). Kinetic modelling of the adsorption of nitrates by ion exchange resin. *Chemical Engineering Journal*, 125,111–117.

Chiu, H.F., Tsai, S.S. & Yang, C.Y. (2007). Nitrate in drinking water and risk of death from bladder cancer: an ecological case-control study in Taiwan. *Journal of Toxicology and Environmental Health, Part A*, *70*(12), 1000–1004.

Demiral, H. & Gündüzoglu, G. (2010). Removal of nitrate from aqueous solutions by activated carbon prepared from sugar beet bagasse. *Bioresource Technology, 101*(6),1675–1680.

Elmidaoui, A., Elhannouni, F., Sahli, M.M., Chay, L., Elabbassi, H., Hafsi, M. & Largeteau, D. (2001). Pollution of nitrate in Moroccan ground water: removal by electrodialysis. *Desalination*, *136*(1–3), 325–332.

Frison, N., Katsou, E., Malamis, S., Bolzonella, D. & Fatone, F. (2013). Biological nutrients removal via nitrite from the supernatant of anaerobic co-digestion using a pilot-scale sequencing batch reactor operating under transient conditions. *Chemical Engineering Journal*, 230, 595–604.

Fu, Z.M., Yang, F.L., An, Y.Y. & Xue, Y. (2009). Characteristics of nitrite and nitrate in situ denitrification in landfill bioreactors. *Bioresource Technology*, *100*(12), 3015–3021.

Husein, D.Z. (2013). Adsorption and removal of mercury ions from aqueous solution using raw and chemically modified Egyptian mandarin peel. *Desalination and Water Treatment, 51*(34-36), 6761-6769.

Husein, D.Z., Al-Radadi, T. & Danish, E.Y. (2016). Adsorption of phosphate using alginate/ zirconium grafted newspaper pellets: Fixed-bed column study and application. *Arabian Journal for Science and Engineering*, *42*(4), 1399–1412. doi: 10.1007/s13369-016-2250-z

Jones, J., Chang, N.B. & Wanielista, M.P. (2015). Reliability analysis of nutrient removal from stormwater runoff with green sorption media under varying influent conditions. *Science of the Total Environment*, 502, 434–447.

Liu, L.,Ji, M., & Wang, F. (2018). Adsorption of Nitrate onto ZnCl2-Modified Coconut Granular Activated Carbon: Kinetics, Characteristics, and Adsorption Dynamics. *Advances in Materials Science and Engineering*, ID 1939032.

Olfs, H.W., Torres-Dorante, L.O., Eckelt, R. & Kosslick, H. (2009). Comparison of different synthesis routes for Mg-Al layered double hydroxides (LDH): characterization of the structural phases and anion exchange properties. *Applied Clay Science*, *43*(3–4), 459–464.

Soares, M.I.M. (2000). Biological denitrification of groundwater. *Water, Air, and Soil Pollution*, *123*(1–4), 183–193.

Taty-Costodes, V.C., Fauduet, H., Porte, C. & Ho, Y.S. (2005). Removal of lead (II) ions from synthetic and real effluents using immobilized Pinus sylvestris sawdust: adsorption on a fixed-bed column. *Journal of Hazardous Materials*, *123*(1–3), 135–44.

Tofighy, M.A. & Mohammadi, T. (2012). Nitrate removal from water using functionalized carbon nanotube sheets. *Chemical Engineering Research and Design, 90*(11), 1815–1822.

Wang, W., Li, M. & Zeng, Q. (2015). Adsorption of chromium (VI) by strong alkaline anion exchange fiber in a fixed-bed column: Experiments and models fitting and evaluating. *Separation and Purification Technology*, 149, 16–23.

Yahaya, N., Abustan, I., Latiff, M. F. P. M., Bello, O. S., & Ahmad, M. A. (2011). Fixed-bed column study for Cu (II) removal from aqueous solutions using rice husk based activated carbon. *International Journal of Engineering and Technology*, *11*(1), 248–252.

Zhu, X., Choo, K.H. & Park, J.M. (2006). Nitrate removal from contaminated water using polyelectrolyte-enhanced ultrafiltration. *Desalination*, *193*(1–3), 350–360.